Final Report

DOE Project: DE-SC-0005399

Linking the uncertainty of low frequency variability in tropical forcing in regional climate change

Chris E. Forest (Principal Investigator)
Department of Meteorology
The Pennsylvania State University

Joseph J. Barsugli (Co-PI)
University of Colorado-Boulder CIRES
and NOAA Earth System Research Laboratory

Wei Li (Co-Investigator)
Department of Meteorology
The Pennsylvania State University

February 20, 2015

Contact Information:

Chris E. Forest
Department of Meteorology
The Pennsylvania State University
507 Walker Building
University Park, PA 16802
ceforest@psu.edu Tel: (814) 865-0710

Table of Contents

1 Project Overview

The project utilizes multiple atmospheric general circulation models (AGCMs) to examine the regional climate sensitivity to tropical sea surface temperature forcing through a series of ensemble experiments. The overall goal for this work is to use the global teleconnection operator (GTO) as a metric to assess the impact of model structural differences on the uncertainties in regional climate variability. To this end, this project covered a four-year period (3 years funded + 1 year no cost extension) of research to address the following three objectives as described in the original proposal:

1) Compute the global teleconnection operator (GTO) that relates a large class of Tropical Sea Surface Temperature (SST) variations to regional climate change response. This is done through the use of idealized perturbed forcing scenarios such as SST anomaly forcing scenarios.
2) Identify and quantify uncertainty in regional climate change related to model physical parameterizations. This is accomplished by analyzing the differences among model-specific GTOs, including models from a perturbed-physics experiment.
3) Develop regional detection and attribution methodology that incorporates the results from objectives (1) and (2) including a comparison of these uncertainties to other uncertainty components.

Primary Outcomes

- We developed a *random perturbation method* (RPM) to estimate the sensitivity of the regional climate change to SST patterns using an AGCM. This method provides alternative estimates of the GTO (Li et al., 2012).
- We applied the RPM method to multiple research areas to investigate the regional climate variability and the contribution of the SST forcing to both the modeled and observed variability. We primarily focused on the climate change response for large-spatial regions (sub-continental) and seasonal-means (Hoffman et al., 2014; Tsai et al., 2014). Additionally, we investigated the large-scale response for northern hemispheric variability on decadal time-scales. (Li and Forest, 2014)
- We investigated the GTO from different AGCMs to identify the impact on the sensitivity matrix due to model structural uncertainty. The GTO experiments we have carried out for this purpose are listed here:

		Models				
Resolutions		CAM3.1	CAM3.5	CAM4.0	CAM5.0	GFDL AM2
	T42	X				
	T85	X				
	FV1.9x2.5	X	X	X	X	X
	T31				X	
	FV0.9x1.25				X	

Main findings

- The random perturbation method was shown to be a useful alternative to previous methods. Both methods have strengths. The RPM is about 12 times more computationally efficient than the original method that was used to investigate the same problem. The increased computational efficiencies also limit the investigations of sensitivity information to larger-spatial scales. (Li et al., 2012)
- Tropical Indian Ocean, Central Pacific and Caribbean Sea are the three primary ocean basins driving the total variability of the North Atlantic Oscillation (NAO) and Pacific-North America (PNA) indices during 1950-2000. (Li and Forest, 2014)
- Variability in dust emissions from the major dust sources can be linked to tropical SST anomalies, particularly in the Indian and western Pacific Oceans. (Hoffman et al., 2014)
- The variability of the regional climate (temperature and precipitation) in tropical river basins can be reasonably captured using the GTO-based analysis of both modeled and observed variability.

2 Methodology for Estimating the GTO

NOTE: The following description of the method follows Li et al. (2012) in describing the estimation of the Global Teleconnection Operator (GTO) for a specific atmospheric GCM.

Although the equations for modeling the climate system are highly nonlinear, it is well established that certain aspects of the climate system can be approximated by a multi-variate linear statistical model. The El Nino-Southern Oscillation (ENSO) phenomenon is remarkably well approximated by a linear stochastic model where the nonlinearities of the real system are all subsumed into the additive noise forcing [*Penland and Sardeshmukh*, 1995]. A linear stochastic model with both additive and multiplicative noise can be used to approximate atmospheric dynamics and fluxes [*Sura et al.*, 2005] and used for medium-range forecasting [*Newman and Sardeshmukh*, 2008]). In all these cases, the complexity of the nonlinear system precludes the computation of the linear approximation from first principles.

2.1. Patch Method

As shown by multiple works, the mean state of the atmospheric response (e.g. seasonal mean) to large scale forcing can be considered as a linear process (*Barsugli and Sardeshmukh*, 2002, hereafter BS02], [*Schneider et al.*, 2003], [*Barsugli et al.*, 2006, hereafter BSS06)], [*Deser and Phillips*, 2006; *Shin et al.*, 2006]). Specifically, the atmospheric response at a given region can be approximated as the sum of the response to each localized SST forcing (i.e. a Green's function as shown in BS02 and

BSS06):

$$\overline{R} \cong K \cdot F = \int K(x) \cdot F(x) dA \tag{1}$$

where $\overline{R}$ is the mean (e.g., seasonal or annual) atmospheric response for a given region, *K(x)* is a linear operator, and *F(x)* is an external large-scale SST forcing at location x with patch area *dA* (see Fig.1). The integral can be approximated as the dot product, **K·F**, where **K** and **F** are vectors representations of linear operator and forcing spatial fields. To estimate *K(x)*, BSS06 set 43 idealized small SST anomaly patches across the tropical Indo-Pacific and Atlantic oceanic regions and estimated the response to the SSTA. "Small" patches are added to the prescribed SST field and ensemble runs are performed for each of these patches. The patches are cosine-squared functions (see BS02) with central amplitudes set to -2ºC and 2ºC with a size (1ºC anomaly contour) of 45ºx22º (longitude x latitude) over the Indo-Pacific ocean and 28ºx22º over Atlantic Ocean. The patches are considered "small" such that the effect on the large-scale circulation is small while being large enough to provide a statistically significant response. The sensitivity of the seasonal mean response at a region of interest (ROI) is defined as the ensemble mean of the regional response per change in SST anomaly at the given location. i.e.:

$$K_{j,i} = \frac{\langle \overline{R}_j \rangle_{warm} - \langle \overline{R}_j \rangle_{cold}}{2 \sum_k F_i^{'}(x_k) dA_{i,k}} \tag{2}$$

where $\langle \overline{R}_j \rangle$ is the ensemble mean of the model response over the *j*th ROI for the ensemble of warm or cold cases. $\sum_k F_i^{'}(x_k) dA_{i,k}$ is the area-integral of the SST anomaly over a given patch *i* on the model grid *k*. By moving the anomaly patch to different locations, the sensitivity of climate change for the ROI can be mapped out across the tropics. Although physically straightforward, this method is computationally expensive (to be defined shortly) by requiring large ensemble sizes for each patch. For example, for a set of 43 SST anomaly patches (as in BS02), if we set the ensemble size at 16 for each warm and cold case (supposing that a 16 member ensemble is sufficient), we require 43x16x2=1376 model runs regardless of the integration time for each run. This drawback motivated us to consider an alternative method to realize the same goal more efficiently.

2.2. Random Perturbation Method

Because the mean state of the atmospheric response to tropical SST forcing could be considered an approximately linear process as shown in BSS02 and BS06, then instead of using the typical Green's function approximation, one can perturb the SST over the entire tropical ocean at once, run a sufficiently large ensemble to obtain the climate system response for many SST anomalies, and estimate the linear operator **K** to get the best estimated response **R**, to the forcing **F**. To clarify, we rewrite equation (1) for a specific region *j* as:

$$\overline{R}_j \cong K_{j,i} \cdot F_i \qquad (3)$$

As written, equation (3) is a linear regression for the regional climate response, R_j, to the SST forcing, F_i, where $K_{j,i}$ is a linear regression coefficient. An error term, e, is also required. To estimate K, we use a random perturbation method (RPM) to generate perturbed SSTA ensembles, which follows methods used in the data assimilation community [*Hawblitzel et al.*, 2007; *Sippel and Zhang*, 2008; *Zhang*, 2005]. The goal is to create an ensemble of random forcing patterns for the entire ocean (or limited region) that can be used to estimate the same sensitivity information obtained by the patch method, and so we need to construct these as follows. To ensure that the regional climate responds to SST anomalies of similar spatial scales, we design the magnitude and size of the random perturbations to be similar to the SST anomaly patches used in the patch method. To match approximately the SST anomaly patch distribution in BS02, we randomly generated 16x16 SST perturbations equally spaced in latitude and longitude across the entire globe and interpolated them to the AGCM model grid resolution (e.g., T42 corresponds to 128x64) using bilinear interpolation. Each point on the 16x16 grid is drawn from a uniform distribution with a range of -2°C–2°C. By design, the perturbations are random in magnitude and uncorrelated in space and across ensemble members. We also consider the randomness of the location of the maximum/minimum perturbation in all sets of ensemble members. As such, we randomly shift the initial coordinate on the 128x64 grid by 1~8 grid points zonally and 1~4 grid points meridionally after doing the interpolation from the coarse coordinate (Note: for T42 resolution, each 16x16 size boxes is composed of 8 grid points in the zonal direction and 4 grid points in the meridional direction). To test whether the random SST perturbations are similar to the perturbations as used by BSS06, we check the auto-correlation across the ensemble of SST perturbations for both a given region and a given point. Both indicate that the perturbed SSTs are a spatially red noise process including small sampling noise and the perturbations are roughly the size of SST anomaly patches in BSS06.

We calculate *K* as the slope of the line that best fits the *R* and *F*:

$$K_{j,i} = \frac{\mathrm{cov}(F_i, \overline{R}_j)}{\sigma^2(F_i)} = \frac{\sigma(\overline{R}_j)\, r(F_i, \overline{R}_j)}{\sigma(F_i)} \qquad (4)$$

where $\mathrm{cov}(F_i, \overline{R}_j)$ is the covariance of the ensemble F_i and $\overline{R}_j$, $r(F_i, \overline{R}_j)$ is the correlation coefficient, and σ is the standard deviation.

Because the regression coefficient *K* for region *j* that correlates with the SST anomaly patch *i* reflects the global teleconnection relation between SST anomaly patches and a given regional climate change, we define the matrix form of K_{ji} as the global teleconnection operator (GTO).

This project first evaluated and verified the two methods from both mathematical and visual images. We then applied the RPM method, which is more computationally efficient, to the estimation of GTO for multiple regions.

3 Model and experimental design

We used the National Center for Atmospheric Research (NCAR) Community Atmospheric Model (CAM) and the GFDL_AM2 AGCM as our simulation tool to examine the impact of model difference on the GTO. The base climatological SST and sea ice boundary dataset (12 months) for all experiments is HadOIBl data averaged from 1982-2001 at the same resolution as the atmospheric component [*McCaa et al.*, 2004].

For the patch method, we generated 43 tropical SST anomaly patches and added them to twelve-month background SST field. For each SST anomaly patch, 32 runs (16 for warm-anomaly and 16-cold anomaly starting from different initial conditions) are performed to get the ensemble response.

For the RPM method, we generated an ensemble of SST perturbation fields over the tropical (30°S-30°N) or global ocean (60°S-60°N) and added them to the model climatological SST field as forcing for the AGCM ensemble simulations. Typically, we used an ensemble size of n=400 while testing to date included an n=1000 member ensemble.

We then forced the model with the updated SST field and performed a branch run starting from year 10 of a 160-year control simulation (we use a 9-year spin-up for the control run to get an equilibrium state). To include uncertainty in initial conditions, we perform 200 branch runs from different starting points with one-year increment (about 50 of the initial conditions has been repeatedly used) and run 20 months for each perturbation field. The model outputs from months 9-20 are used to calculate the seasonal mean response for any variable at a given model location (or for any diagnostic estimated from the model response).

4 Overview of Key Results

4.1 Verification of RPM and Patch method

4.1.1 Teleconnection pattern response to an individual SST anomaly patch

Teleconnection pattern response to an individual SST anomaly patch

As a standard example, we examined the ensemble-mean model response for a specific SST anomaly patch over the central Pacific Ocean (187.5E, 5.6S, ~200km north of Atafu Island) to compare the two methods. For the seasonal large-scale (global or hemispheric spatial scale) response, the two methods are roughly equivalent in terms of the sensitivity of the temperature to SST anomaly patch at a specific location (Fig. 1). The slope of the linear fit provides the estimate of K_{ij} in equation (2) and we see good agreement between the patch and RPM approaches.

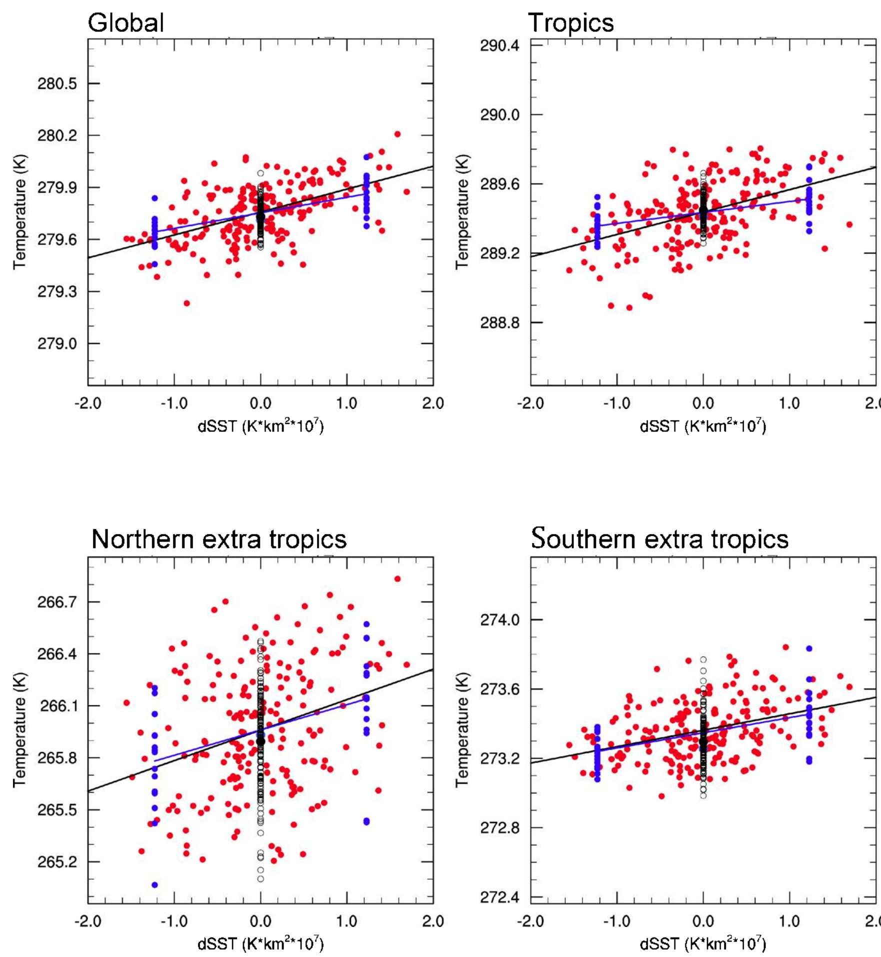

Figure 1: Scatter plots of the winter (DJF) regional mean T850 against SST anomaly integrated over one patch region (centered at 187.5E, 5.6S with dimension of 45ºx22º). Red dots denote the response from a 200-member ensemble using the RPM, blue dots are the 32-member ensemble response from the patch method. Black and blue regression lines are shown for both cases. Black open circles are the T850 at initial conditions for 200-ensemble runs of RPM. Black solid dot is the mean T850 of the 200 initial conditions for RPM. Blue solid dot is the mean T850 of the 32 initial conditions for patch run. The temperature range for all cases is 2K.

We estimate the teleconnection pattern driven by an elevated mean SST anomaly for the Nino4 region and the simulated temperature at 850hPa for the global domain (Fig.2) to compare the two methods. Although obtained by setting random perturbation across the entire tropical region (RPM), it shows strong similarity to the same result obtained from the ensemble mean of the response to a single patch over same Niño4 region (i.e. patch method) (Fig. 2a,c). The patterns indicate consistency of the teleconnection relation between a local SST anomaly and global response from the dynamical perspective and statistical point of view.

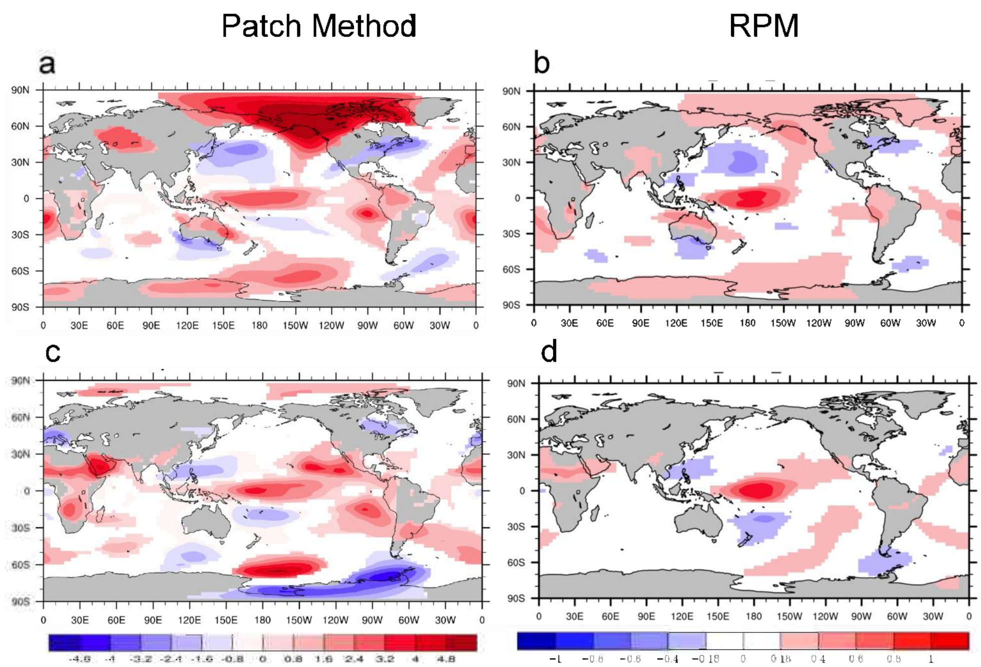

Fig.2 Comparison of temperature at 850hPa forced by SST anomaly patch over ~NiNO4 through patch method (a and c. unit :K) and correlation between regional mean SST anomaly over NiNO4 and global T850 (b and d) through RPM for different seasons (a and b: DJF; c and d: JJA). Only regions passing a 95% significance test are mapped. (RPM ensemble n=200).

4.1.2 Sensitivity to tropical SST anomalies: the Global Teleconnection Operator

We present the GTO (i.e. the sensitivity of regional response to tropical SST anomaly, dR/dT_{patch}) for T850 and precipitation averaged over three regions to show the consistency of the two methods. The results indicate only the ocean region corresponding to the tropical SSTs where the patch method was developed.

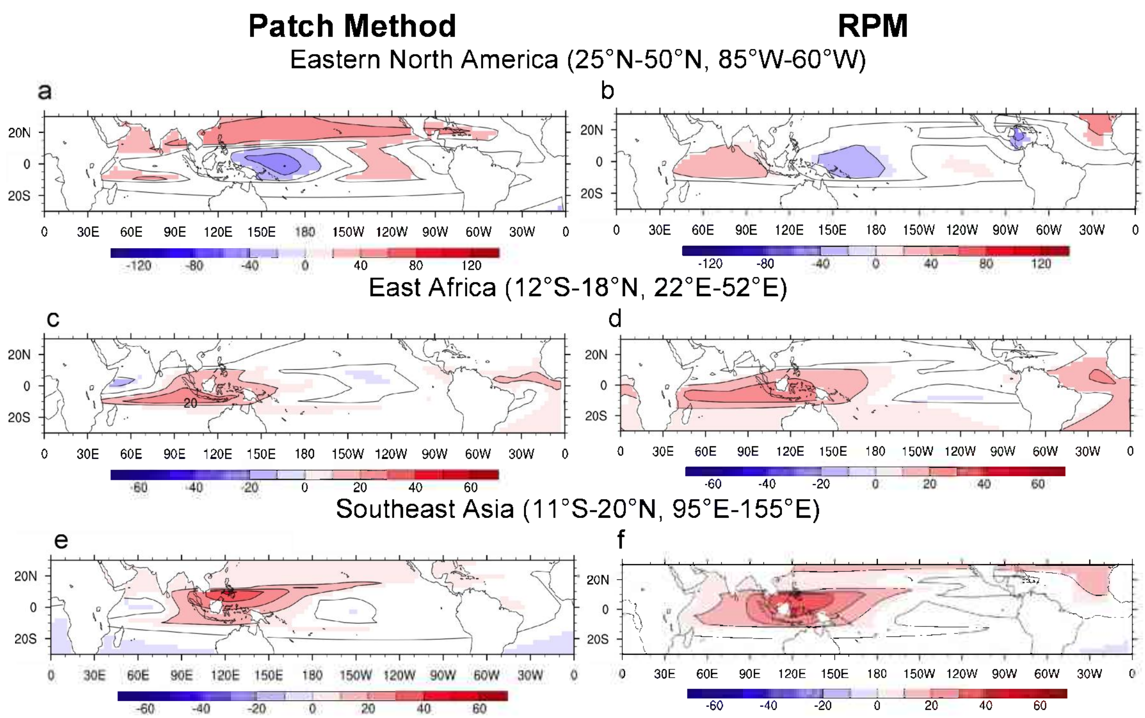

Figure 3: Comparison of sensitivity map of winter (DJF) T850 over different target regions: Eastern North America; East Africa, and Southeast Asia from Patch method (a,c,e) and RPM (b,d,f). (RPM ensemble for n=200.) Shaded regions denote the regions passing a 20% significance test. Units: K/(K·10^7·km^2).

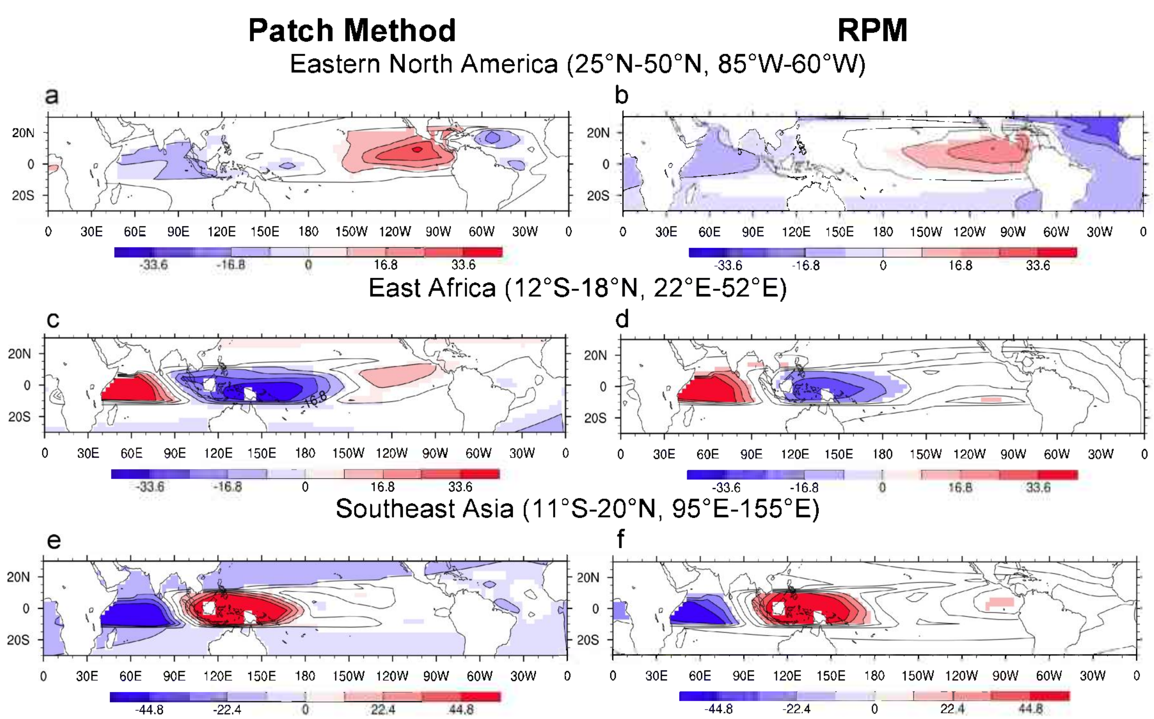

Figure 4: Same as Fig. 3 but for DJF precipitation. Units: mm/(K·10^7·km^2).

5 Results: Impact of Model Differences on GTO Estimates

The assessment of the GTO for different models is an important task to be used as a metric for model behaviors as identified in the original project goals. This task requires assessing the regional climate variability in addition to estimating the changes in the variability due to the teleconnections estimated with the GTO. At the end of the project, a first summary paper is nearly complete with some additional analysis required to assess statistical significance of estimated changes. The primary findings of the initial analysis are presented here. We compare the GTO results for different versions of the models (Section 5.1.1), for different resolutions of the same model (Section 5.1.2), and for different dynamical cores with the same model (not shown).

5.1.1 Dependence on physical parameterizations

We chose three options for presenting the differences due to alternate versions of the NCAR CAM. First, we show the overall variability estimates for the four models across the regions for the ensemble in Fig. 5. Second, we show the different sensitivity estimates for regional and global-mean T850 in Fig. 6. Third, we highlight the GTO spatial patterns for four regions of interest for climate impacts research.

To estimate the overall variability, we use the standard deviation of the seasonal response of the 200-member ensemble runs forced with different perturbed SST and initial conditions to define the ensemble variability of the seasonal response (i.e. variability of perturbed SST and internal variability). We use the standard deviation of the seasonal response of control runs forced with climatological SST during years 10 to 109, which was used as initial conditions for the perturbed ensemble run, to define the internal unforced variability. As shown in Figures 5 and 6, the regional response shows varying sensitivity to perturbed SST forcing and internal variability. (We note that the differences in the estimated variability across the four models are typically small compared to the overall estimated internal variability.) Generally, as is expected, the global and hemispheric scale responses have smaller sensitivities than the continental scale responses. Seasonal mean temperatures over some of the extra-tropical regions in northern hemisphere, such as Alaska, North America and Asia are more sensitive to SST perturbation and exhibit larger internal variability.

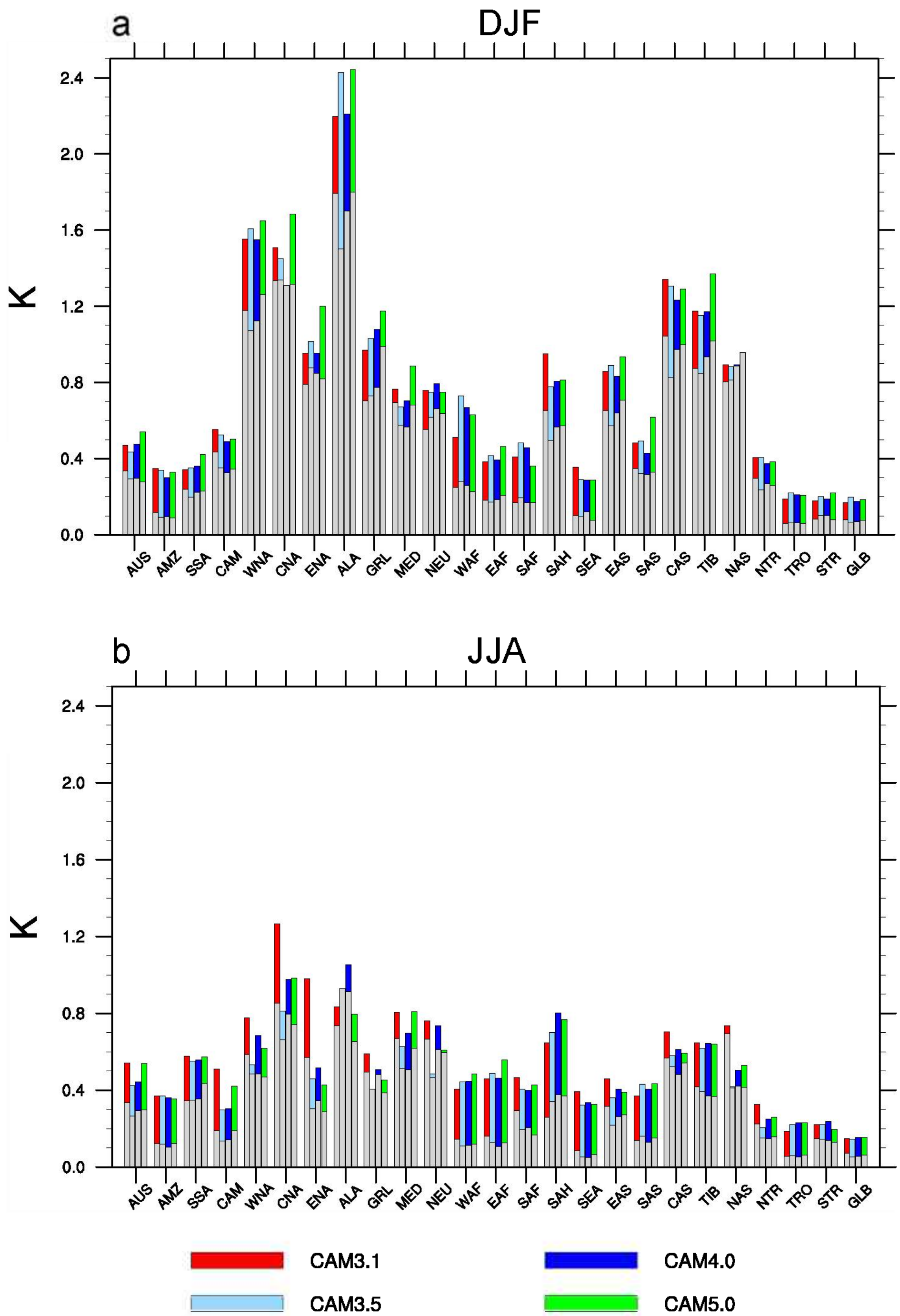

Figure 5: Ensemble standard deviation of the regional mean temperature at 850 hPa of perturbed SST run by CAM3.1, CAM3.5, CAM4.0 and CAM5.0 during a).Winter (December – January) and b). Summer (June – August). Grey bars are the ensemble standard deviation of the control run without perturbed SST. Ensemble size, n=200.

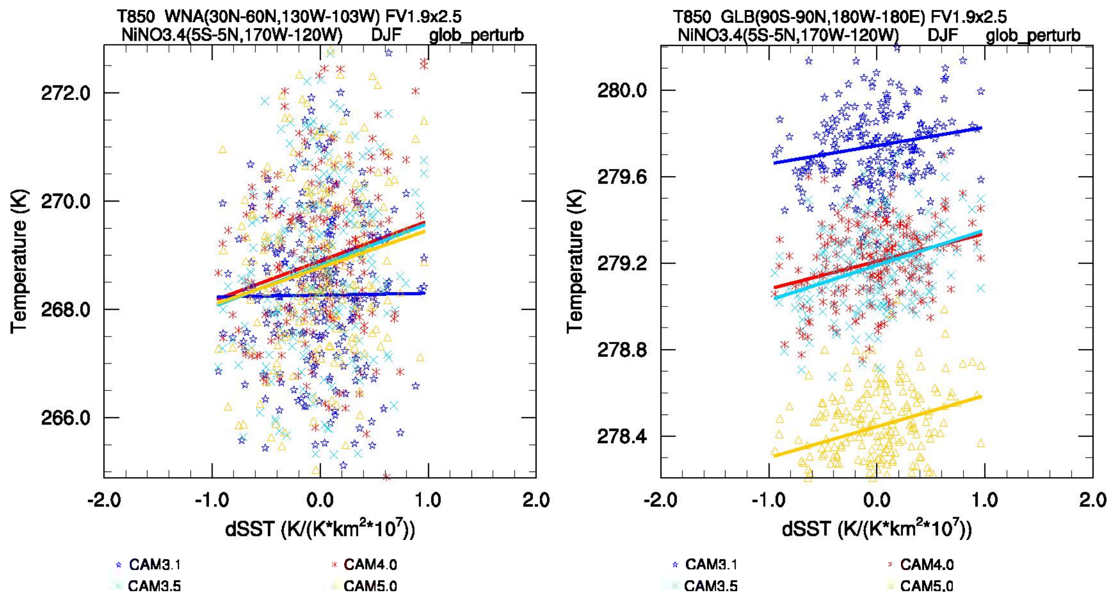

Figure 6: Scatter plots of the regional response (T850) as a function of SST anomaly patch over the NiNO3.4 region from four CAMs: CAM3.1 (Dark blue), CAM3.5 (Light Blue), CAM4.0 (Red), and CAM5.0 (Yellow). Note: The global mean temperatures for the four models are not the same despite being driven by the same climatological SST fields.)

Fig.7 shows the geographical distribution of GTO by different model versions for regions with large variability as shown in Fig.5. From EQ(1), the pattern and sign of GTO reflect the simultaneous correlation between regional response and SST perturbation with the magnitude modified by the variability of the regional response. Generally GTO patterns are consistent across the four models in that they all capture the correlation structures between the response and tropical SST anomalies to different extents. Relatively larger model discrepancies occur in CAM3.1 simulation of T850 sensitivity for western North America, in which negative correlations for the Indian Ocean are missed; for Eastern North America where the signal over the north Pacific ocean is missed; for Greenland where the signal over the western Pacific is weaker; and for the Mediterranean Basin where correlations over the north Pacific are emphasized. Relatively larger model discrepancies also occur in the CAM3.1 simulation of precipitation sensitivity over Central North America where in the Indian Ocean, the signal weakens while in the northeast Pacific and Atlantic, the signals are stronger. So that we do not only single out CAM3.1, other CAM versions also show different GTO patterns when compared with other model versions. For example, CAM4.0 simulations over Tibet miss the GTO signal for temperature sensitivities in the western Pacific. Plus, the CAM3.5 simulation over East Asia misses the signal of east Pacific for summer precipitation.

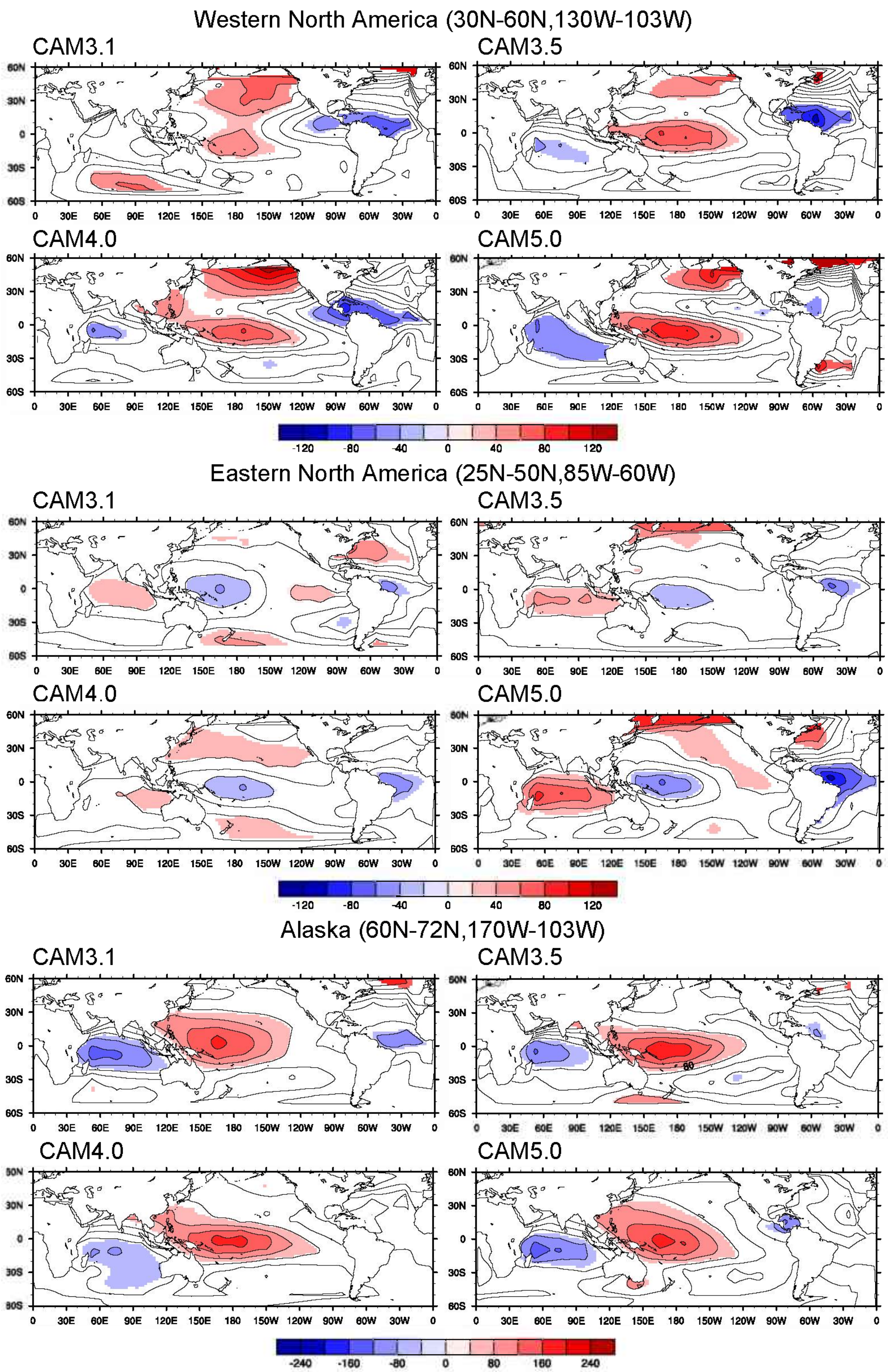

Fig. 7 Geographical distribution of GTO for T850 during DJF by CAM3.1, CAM3.5, CAM4.0 and CAM5.0 (two-tail T- test with significance level of 20% has been performed to mask out the insignificant regions, units: $K/(K \cdot 10^7 \cdot km^2)$).

5.1.2 Dependence on Model Resolution

Fig. 8 shows the ensemble variability of 200 perturbed SST runs for different regions from CAM3.1 T42 and T85. Generally the changes due to different resolutions between each bar are smaller than the changes due to different models (see Fig. 5). When compared with Figure 5, the seasonal responses for some regions are sensitive to both resolution difference and model difference.

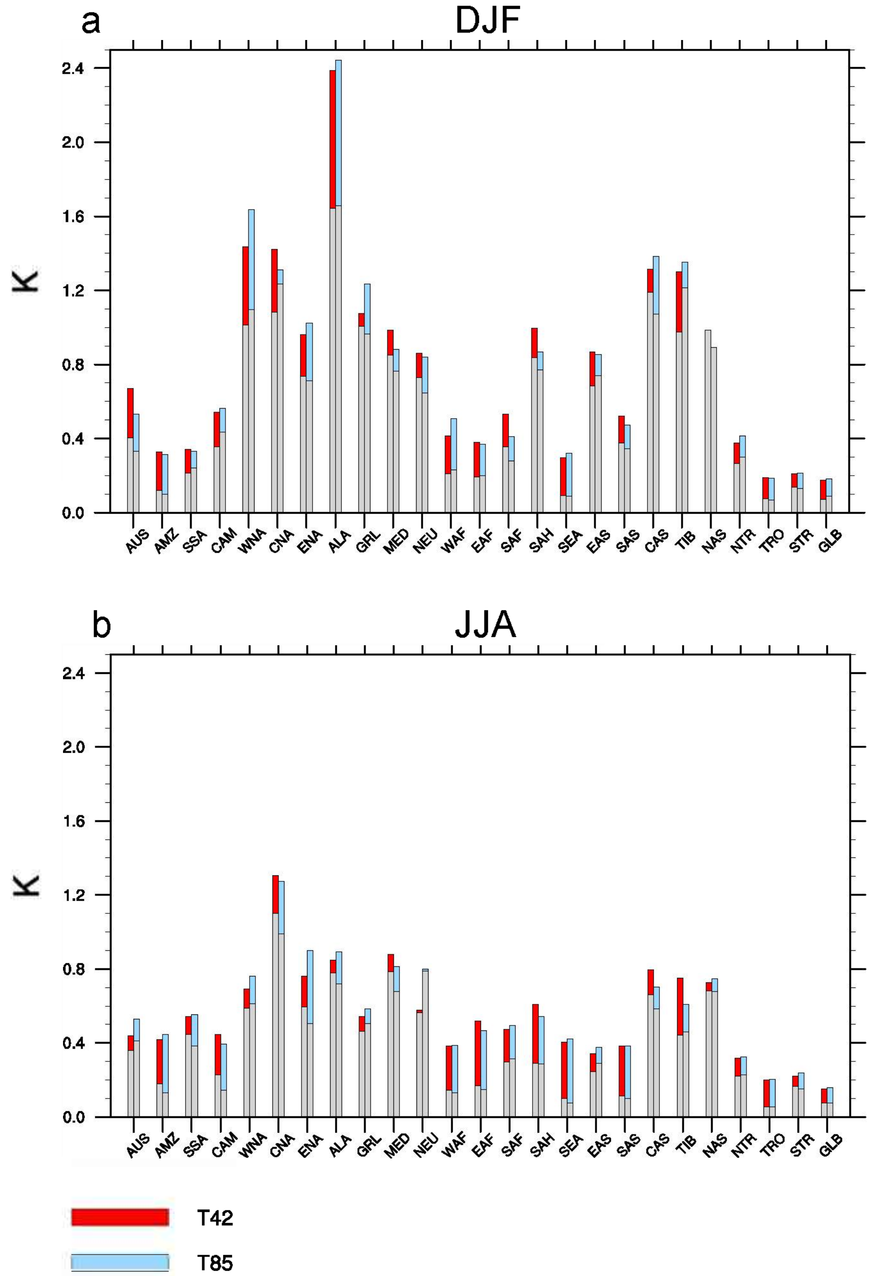

Figure 8: Same as Fig.5, but for CAM3.1 simulations with T42 and T85 resolutions.

The correlation patterns between the regional climate and SST perturbation are generally consistent for different model resolution. Relatively larger discrepancies occur over the eastern North America in which correlation pattern of temperature over Pacific and Indian Ocean shift slightly. Such shifts in the pattern also occur over the central north America in summer precipitation simulation. The discrepancies in the correlation patterns over certain regions should be considered carefully because they can confound our understanding of the impact due to regional SST changes in regional climate changes that are not distinct from the changes due to different model resolutions. A careful assessment of the statistical significance of these results requires further investigation.

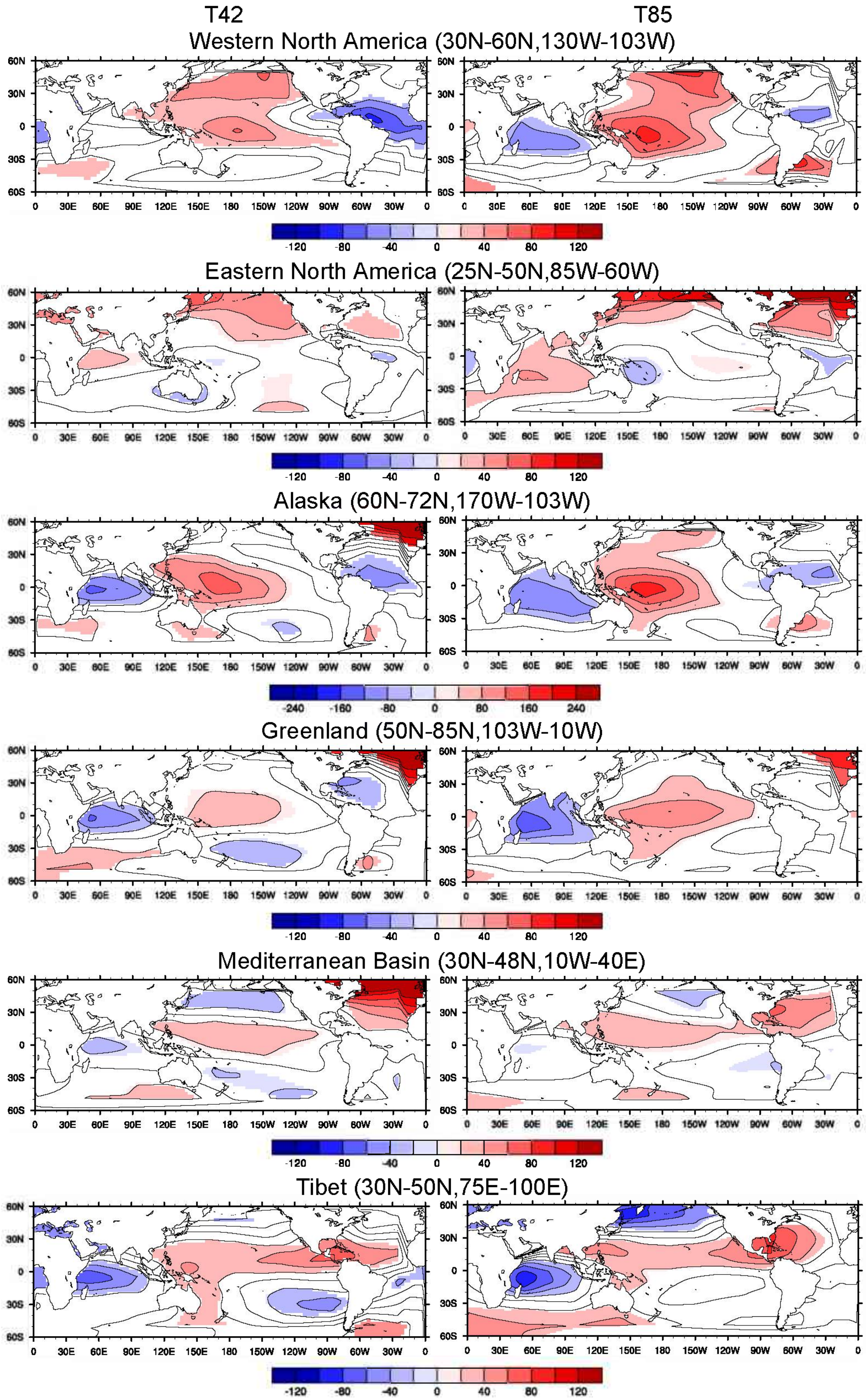

Figure 9: Geographical distribution of GTO during DJF by CAM3.1 T42 and T85.

6 Results: Understanding Regional Climate Change using the GTO Method

Three papers have been accepted in peer-reviewed journals directly from this project. Several papers are in preparation at this time related to the multiple models work and related to using the GTO to identify sensitivity to model structural differences. These papers-in-prep have required additional simulations beyond the scope of the original research.

The following three abstracts are from the respective papers to indicate the breadth of the tool when applied to understanding the sensitivity of specific climatic features being driven by SST variability.

6.1 Sensitivity of Emissions Source Regions to SST Variability

Citation: Hoffman, A. L., C. E. Forest, and W. Li (2014), Estimating the sensitivity of regional dust sources to sea surface temperature patterns, *J. Geophys. Res. Atmos., 119*, 10,160–10,174, doi:10.1002/2014JD021682.

Abstract: Exploring the impact of sea surface temperature (SST) anomaly patterns on local climate in major dust source regions helps clarify our understanding of variability in the global dust cycle. In contrast to previous work, this research focuses explicitly on the influence of SST anomalies on dust emissions and attempts to explain the mechanisms by which SST anomalies affect seasonal dust emissions. This study investigates the seasonal sensitivity of mineral aerosol emissions to SST anomaly patterns from the Bodele Depression, West Africa, Sahel, Kalahari Desert, Arabian Desert, and Lake Eyre basin. The global teleconnection operator, which relates regional climate responses to SST anomaly patterns, is estimated for relevant variables in an ensemble of the National Center for Atmospheric Research Community Atmosphere Model version 5 forced by randomly perturbed climatological SST fields. Variability in dust emissions from major dust sources is linked to tropical SST anomalies, particularly in the Indian and western Pacific Oceans. Teleconnections excited by remote SST anomalies typically impact dust emissions via changes in near-surface wind speeds and friction velocity. However, SST-driven impacts on the threshold friction velocity can be of the same order of magnitude as changes in the friction velocity, suggesting the impact of SST anomalies on precipitation and soil moisture is also significant. Identifying SST anomaly patterns as a component of internal variability in regional dust emissions helps characterize human influences on the dust cycle as well as improve predictions of climate, nutrient cycles, and human environments.

6.2 *Sensitivity of River Basin Climatology for Hydrologic Research to SST Variability*

Citation: Tsai, C.-Y., C. E. Forest , and T. Wagener, 2014: On the use of SST-forced teleconnection patterns to estimate precipitation effects on regional river basins, *Clim. Dynamics*, DOI 10.1007/s00382-014-2449-1.

Abstract: We investigate how to identify and assess teleconnection signals between anomalous patterns of sea surface temperature (SST) changes and climate variables related to hydrologic impacts over different river basins. The regional climate sensitivity to tropical SST anomaly patterns is examined through a linear relationship given by the global teleconnection operator (GTO, also generally called a sensitivity matrix or an empirical Green's function). We assume that the GTO defines a multilinear relation between SST forcing and regional climate response of a target area. The sensitivities are computed based on data from a large ensemble of simulations using the NCAR Community Atmospheric Model version 3.1 (CAM 3.1). The linear approximation is evaluated by comparing the linearly reconstructed response with both the results from the full non-linear atmospheric model and observational data. The results show that the linear approximation can capture regional climate variability that the CAM 3.1 AMIP-style simulations produce at seasonal scales for multiple river basins. The linear method can be used potentially for estimating drought conditions, river flow forecasting, and agricultural water management problems.

6.3 *Sensitivity to SST Variability of Northern Hemisphere Large-scale Variability in the North Atlantic Oscillation and the Pacific-North America Patterns*

Citation: Li, W. and C. E. Forest, 2014: Estimating the sensitivity of the atmospheric teleconnection patterns to SST anomalies using a linear statistical method. J. Climate, 27, 9065–9081. doi: 10.1175/JCLI-D-14-00231.1.

Abstract: The Pacific–North American (PNA) pattern and the North Atlantic Oscillation (NAO) are known to contain a tropical sea surface temperature (SST)-forced component. This study examines the sensitivity of the wintertime NAO and PNA to patterns of tropical SST anomalies using a linear statistical–dynamic method. The NAO index is sensitive to SST anomalies over the tropical Indian Ocean, the central Pacific Ocean, and the Caribbean Sea, and the PNA index is sensitive to SST anomalies over the tropical Pacific and Indian Oceans. The NAO and PNA patterns can be reproduced well by combining the linear operator with the consistent SST anomaly over the Indian Ocean and the Niño-4 regions, respectively, suggesting that these are the most efficient ocean basins that force the teleconnection patterns. During the period of 1950–2000, the NAO time series reconstructed by using SST anomalies over the Indian Ocean + Niño-4 region + Caribbean Sea or the Indian Ocean + Niño-4 region is significantly correlated with the observation. Using a cross-

spectral analysis, the NAO index is coherent with the SST forcing over the Indian Ocean at a significant 3-yr period and a less significant 10-yr period, with the Indian Ocean SST leading by about a quarter phase. Unsurprisingly, the PNA index is most coherent with the Niño-4 SST at 4–5-yr periods. When compared with the observation, the NAO variability from the linear reconstruction is better reproduced than that of the coupled model, which is better than the Atmospheric Model Intercomparison Project (AMIP) run, while the PNA variability from the AMIP simulations is better than that of the reconstruction, which is better than the coupled model run.

7 Conclusion

Based on the original project plan and the completed work, we have made significant progress in multiple areas of the intended research. Our effort has produced 6 published works (4 peer reviewed papers and 2 MS theses) and we have presented these results in 23 presentations over the past 4 years. Two students, Alexis Hoffman and Chii-Yun Tsai, have graduated with MS degrees and are continuing to pursue PhD degrees. Dr. Wei Li completed her post-doctoral training and is now employed working at NCEP with NOAA.

The computational component of the project was a strong success in proving that a standardized teleconnection response can be identified in multiple models with a modest number of simulation years (~2000) and suggests that the broader climate modeling community can implement this model diagnostic approach, with little effort.

From the scientific perspective, we have demonstrated the utility of the approach for interpreting regional sensitivities in a specific controlled set of experiments. This approach can be extended to other forcing scenarios for land surface changes and for changes in the polar sea-ice coverage to further investigate the relative role of the forced teleconnection response as being separate from the internal variability of the full coupled climate system.

The GTO method has two significant directions to pursue. First, the method provides a potential tool for statistical emulation of the regional climate response to SST variability. Second, the method can be used to calibrate parameterizations in the model that have a dependence on the regional climate state (which can be impacted by errors in SST driven teleconnections).

Here are the Main Findings (repeated from Section 1.)

- The random perturbation method was shown to be a useful alternative to previous methods. Both methods have strengths. The RPM is about 12 times more computationally efficient than the original method that was used to investigate the same problem. The increased computational efficiencies also limit the investigations of sensitivity information to larger-spatial scales. (Li et al., 2012)
- Tropical Indian Ocean, Central Pacific and Caribbean Sea are the three primary ocean basins driving the total variability of the North Atlantic Oscillation (NAO) and Pacific-North America (PNA) indices during 1950-2000. (Li and Forest, 2014)

- Variability in dust emissions from the major dust sources can be linked to tropical SST anomalies, particularly in the Indian and western Pacific Oceans. (Hoffman et al., 2014)
- The variability of the regional climate (temperature and precipitation) in tropical river basins can be reasonably captured using the GTO-based analysis of both modeled and observed variability.

8 Publications

Peer-reviewed Articles

1. Li, W., C. E. Forest, and J. Barsugli, 2012: Comparing two methods to estimate the sensitivity of regional climate simulations to tropical SST anomalies, *J. Geophys. Res.*, 117, D20103, doi:10.1029/2011JD017186.

2. Tsai, C.-Y., C. E. Forest , and T. Wagener, 2014: On the use of SST-forced teleconnection patterns to estimate precipitation effects on regional river basins, *Clim. Dynamics*, DOI 10.1007/s00382-014-2449-1.

3. Hoffman A. L., C. E. Forest, W. Li, 2014: On the use of SST-forced teleconnection patterns to estimate dust emissions and depositions at sub-continental scales, *J. Geophys. Res.- Atmos.*, DOI: 10.1002/2014JD021682.

4. Li, W. and C. E. Forest, 2014: Estimating the sensitivity of the atmospheric teleconnection patterns to SST anomalies using a linear statistical method. *J. Climate*, 27, 9065–9081. doi: 10.1175/JCLI-D-14-00231.1.

5. Chris E. Forest, Wei Li and Joseph Barsugli, 2015: Estimating the structral uncertainty in modeling of sensitivity of regional climate to SST forcing. Prepared for submission to *J. Geophys. Res*.

Theses

1. Chii-Yun Tsai, 2013: Estimating the regional climate responses over river basins to changes in tropical sea surface temperature patterns, MS Thesis, The Pennsylvania State University.

2. Alexis L. Hoffman, 2013: Estimating the sensitivity of regional dust sources to sea surface temperature patterns, MS Thesis, The Pennsylvania State University.

9 Presentations

In Chronological Order:

2010

Exploring sensitivity of regional information from global climate models to model resolution and structure
C.E. Forest and W. Li
Geophysical Research Abstracts, 12:EGU2010-11746
EGU General Assembly
April 2010

Identifying Model Uncertainty in Regional Climate Predictions from Multiple Versions of NCAR CAM
Chris E. Forest
MIT Atmospheric Science Seminar
MIT, Cambridge, MA
September 27, 2010.

Quantifying uncertainty of simulations from NCAR Community Atmospheric Models at regional scales
C.E. Forest, W. Li, and J.J. Barsugli
Abstract GC22B-07
AGU Fall Meeting
December 2010

2011

Assessing uncertainty of regional climate change from global climate models
C.E. Forest, W. Li, and J.J. Barsugli
AMS 23rd Conference on Climate Variability and Change Paper 3B.6
Seattle, WA
January 2011

Linking the uncertainty of low frequency variability in tropical forcing to regional climate change
Chris E. Forest, Wei Li, Joe Barsugli
DOE CESM PI Meeting
Washington, DC
Sept 19-22, 2011

Comparing methods for estimating sensitivity of regional climate change to SST anomaly from multiple AGCMs
C.E. Forest, W. Li, J.J. Barsugli
Abstract ID: GC11B-0911
AGU Fall Meeting
December 2011

Sensitivity of regional climate change predictions to SST anomaly patterns for present-day and future scenarios
W. Li, C.E. Forest, J.J. Barsugli
Abstract ID: GC11A-0896
AGU Fall Meeting
December 2011

Assessing model uncertainty in regional climate predictions: Using metrics based on global atmospheric responses to SST patterns
Chris E. Forest
Earth and Atmospheric Sciences Seminar
Cornell University, Ithaca, NY
October 19, 2011.

Assessing model uncertainty in regional climate predictions: Using metrics based on global atmospheric responses to SST patterns
Chris E. Forest
Department of Atmosphere, Ocean, and Planetary Physics Informal Talk
Oxford University, UK
September 28, 2011.

2012

Uncertainty quantification of regional climate change based on structural uncertainty in atmospheric GCMs (Invited)
C.E. Forest and W. Li
Abstract ID: GC31C-08
AGU Fall Meeting
December 2012

Assessing the teleconnection effect on the regional climate change using a linear response to SST patterns
W. Li, C.E. Forest, and J.J. Barsugli
Abstract ID: GC43E-1079
AGU Fall Meeting
December 2012

2013

Exploring effects of different dynamical cores in global climate models on regional predictions.
Chris E Forest, Wei Li, Joseph Barsugli
GPC Mini-Symposium: Global Climate Models: Dynamical Cores, Strengths and Weaknesses
APS Division of Fluid Dynamics Meeting
Pittsburgh, PA
November 26, 2013

Estimating the Regional Climate Responses over River Basins to Changes in Tropical Sea Surface Temperature Patterns
Chii-Yun Tsai, Chris E. Forest, Thorsten Wagener
AGU Fall Meeting
Abstract ID: A21B-0014
December 12, 2013.

Estimating the Impact of Sea Surface Temperature Patterns on Mineral Aerosol Emission and Deposition
Alexis Hoffman, Chris Forest, and Wei Li
AGU Fall Meeting
Abstract ID: A41G-0141
December 12, 2013.

Where is the tropical ocean important for the low-frequency variability of the atmospheric teleconnection patterns? A perspective from a linear statistical model
Wei Li and Chris E. Forest
AGU Fall Meeting
Abstract ID: GC51D-1009
December 13, 2013.

Linking SST Changes to River Flow; Linking River Flow and IAMs
Chris E. Forest, Chii-Yun Tsai, Wei Li, Thorsten Wagener
DOE PIAMDDI Project Meeting
Stanford University
December 13, 2013.

Building emulators across model hierarchies
Chris E. Forest, Alex Libardoni, Ashley Warner, Randy Miller, Klaus Keller,
DOE PIAMDDI Project Meeting
Stanford University
December 13, 2013.

2014

Discussant in Probabilistic information on potential climate futures
Chris E Forest
NEEDS FOR SCENARIOS: SCIENCE, ASSESSMENTS AND DECISIONMAKING
ENERGY MODELING FORUM
Workshop on Climate Change Impacts and Integrated Assessment (CCI/IA)
30 July 2014
Snowmass, Colorado

Equilibrium Climate Sensitivity: A discussion of the IPCC AR5 estimates and some recent results
Chris E Forest
CPEP Weekly Seminar
University of Wisconsin-Madison
February 28, 2014

Global Teleconnection Operators: A method for assessing regional climate sensitivities
Chris E Forest, Wei Li, Judy Tsai, Alexis Hoffman, Joseph Barsugli
AOS Department Colloquium
University of Wisconsin-Madison
March 3, 2014

Uncertainty quantification of regional climate change based on structural uncertainty in atmospheric GCMs
Chris E. Forest, Wei Li, Chii-Yun Tsai, Alexis Hoffman, Joseph Barsugli, Thorsten Wagener, Erwan Monier
DOE PI Meeting
May 13, 2014

Characterizing Uncertainty in Climate Change from Global to Regional Scales
Chris E Forest, Alex Libardoni, Ashley Warner, Klaus Keller, Wei Li, Judy Tsai, Alexis Hoffman, Joseph Barsugli
Environmental & Water Resources Distinguished Speaker Seminar Series
Cornell University
Oct 28, 2014

2015

On using global teleconnection operators (GTOs) for attribution of climate events
Chris E Forest and Judy Tsai
IDAG Meeting 2015
NCAR, Boulder, Colorado
January 25, 2015

10 References

Barsugli, J. J., and P. D. Sardeshmukh (2002), Global atmospheric sensitivity to tropical SST anomalies throughout the Indo-Pacific basin, *J Climate*, *15*(23), 3427-3442.

Barsugli, J. J., S. I. Shin, and P. D. Sardeshmukh (2006), Sensitivity of global warming to the pattern of tropical ocean warming, *Clim Dynam*, *27*(5), 483-492.

Deser, C., and A. S. Phillips (2006), Simulation of the 1976/77 climate transition over the North Pacific: Sensitivity to tropical forcing, *J Climate*, *19*(23), 6170-6180.

Hawblitzel, D. P., F. Q. Zhang, Z. Y. Meng, and C. A. Davis (2007), Probabilistic evaluation of the dynamics and predictability of the mesoscale convective vortex of 10-13 June 2003, *MONTHLY WEATHER REVIEW*, *135*(4), 1544-1563.

McCaa, J. R., M. Rothstein, B.E. Eeaton, J.M. Rosinski, and M. Vertenstein (2004), User's guide to the NCAR Community Atmosphere Model (CAM3.0)*Rep.*, Climate And Global Dynamics Division, National Center For Atmospheric Research, Boulder, Colorado, USA.

Newman, M., and P. D. Sardeshmukh (2008), Tropical and stratospheric influences on extratropical short-term climate variability, *J Climate*, *21*(17), 4326-4347.

Penland, C., and P. D. Sardeshmukh (1995), The Optimal-Growth of Tropical Sea-Surface Temperature Anomalies, *J Climate*, *8*(8), 1999-2024.

Schneider, E. K., L. Bengtsson, and Z. Z. Hu (2003), Forcing of Northern Hemisphere climate trends, *J Atmos Sci*, *60*(12), 1504-1521.

Sippel, J. A., and F. Q. Zhang (2008), A Probabilistic Analysis of the Dynamics and Predictability of Tropical Cyclogenesis, *JOURNAL OF THE ATMOSPHERIC SCIENCES*, *65*(11), 3440-3459.

Sura, P., M. Newman, C. Penland, and P. Sardeshmukh (2005), Multiplicative noise and non-gaussianity: A paradigm for atmospheric regimes, *J Atmos Sci*, *62*(5), 1391-1409.

Zhang, F. (2005), Dynamics and Structure of Mesoscale Error Covariance of a Winter Cyclone Estimated through Short-Range Ensemble Forecasts, *MONTHLY WEATHER REVIEW*, *133*, 2876-2893.